

# Fracture of Rock-Concrete Interfaces: Laboratory Tests and Applications

by J. M. Chandra Kishen and Victor E. Saouma

*The fundamental understanding of the fracture behavior at the rock-concrete interface requires evaluation of the fracture energy, which is an interface material property. As in concrete or rock, fracture at the interface is characterized by a steady degradation of its structure. With increasing degradation of the material (opening of the crack), less stress is transferred across the interface until it is completely separated. The interface undergoes tensile softening. Wedge-splitting tests are performed on the limestone-concrete interface to evaluate the Mode I fracture energy. These experiments are followed by linear and nonlinear fracture mechanics based on numerical analysis to obtain the fracture toughness. The fracture parameters so obtained are used in the fracture mechanics-based analysis of a gravity dam for the determination of crack length between the concrete dam and rock foundation.*

**Keywords:** concrete; fracture; toughness.

## INTRODUCTION

Dam safety programs are of utmost importance to society and call for combined use of multidisciplinary efforts. The concept of safety should apply not only to the preplanning stages of design but also to the post-operational and maintenance stages. Due to this, recent years have witnessed a major research interest from the academic community in fracture mechanics of concrete and a high concern from the engineering community and power utility companies owning dams, in dam safety.

From recent studies,<sup>1</sup> it is well understood that the concepts of fracture mechanics could be usefully applied for the failure analysis of concrete dams. In a concrete dam, the interface between the concrete superstructure and the rock foundation is one of the potential sites of crack formation and subsequent failure. Not only do they contribute in weakening the mechanical strength, but they also constitute conduits for water to seep through and exert uplift pressure. Hence, it is important that proper mechanical behavior of this interface is understood in light of realistic loading conditions.

The fracture mode at an interface of dissimilar materials is often mixed. Differences between elastic properties across an interface will generally disrupt the symmetry even when the geometry and loading are otherwise symmetric with respect to the crack. Mixed mode crack propagation involves the presence of in-plane normal and shearing tractions near the front of an existing crack (notch). The stress and displacement fields near the tip of a crack present between dissimilar materials are given in the Appendix. The Federal Energy Regulation Commission (FERC) guidelines<sup>2</sup> for the evaluation of hydroelectric projects include provisions addressing the use of finite element analysis instead of hand calculation methods. Therefore, besides theoretical considerations, valid fracture mechanics material properties should be determined for dam concrete-rock foundation interface for the use in fracture

mechanics-based finite element models. Hence, it is vitally important to conduct experiments on interface specimens to extract valid material properties.

This paper presents the wedge-splitting test<sup>3</sup> performed on rock-concrete interface specimens. The specific fracture energy  $G_F$ , which is the energy required to fracture a unit area of the interface, is evaluated. In addition, numerical analyses are performed on these wedge-splitting specimens using the concepts of linear and nonlinear fracture mechanics to obtain the fracture toughness. Further, the fracture parameter obtained in the wedge-splitting tests and their numerical analysis is used in the analysis of the Greyrock gravity dam for determining the crack length at the dam-foundation interface.

## RESEARCH SIGNIFICANCE

In this paper, the specific fracture energy, which is the energy required to fracture a unit area, is determined experimentally for cracks at the concrete-limestone interface. Further, through a numerical compliance analysis, the Mode I and Mode II fracture toughnesses are computed. The fracture toughness and the fracture energy serve as principal fracture properties in most of the linear and nonlinear fracture mechanics-based numerical models, respectively.

## EXPERIMENTAL PROCEDURE

### Test specimen

The geometry of the wedge-splitting specimen is shown in Fig. 1. One half of this specimen is rock while the other half is concrete. The type of rock used is Indiana limestone. The limestone portion was machine-cut to its corresponding size and was placed on its side inside a mold. Freshly mixed concrete (cement:sand:coarse aggregate:water = 1:2.2:2.8:0.45) was placed over the limestone, thus providing a cold-jointed interface. Before casting the concrete portion, the interface portion of limestone was cleaned with a wire brush. The molds were stripped after 2 days following casting and the specimens were cured in a fog room with 100% humidity for more than 21 days. A total of 12 specimens was prepared.

The experiments were conducted in a closed-loop servo-hydraulic testing machine under crack mouth opening displacement (CMOD) control. The rate of CMOD was maintained around  $1.4 \times 10^{-4}$  mm/s. The CMOD was monitored using a clip gage, fixed at a level, where the resultant splitting force acted on the specimen. A representative load versus CMOD response diagram<sup>4</sup> is shown in Fig. 2. In this figure, it is seen that unloading-reloading was performed at

ACI Structural Journal, V. 101, No. 3, May-June 2004.

MS No. 02-455 received December 9, 2002, and reviewed under Institute publication policies. Copyright © 2004, American Concrete Institute. All rights reserved, including the making of copies unless permission is obtained from the copyright proprietors. Pertinent discussion including author's closure, if any, will be published in the March-April 2005 ACI Structural Journal if the discussion is received by November 1, 2004.

**J. M. Chandra Kishen** is an assistant professor of civil engineering at the Indian Institute of Science, Bangalore, India. He received his PhD from the University of Colorado at Boulder, Boulder, Colo., in 1996. His research interests include the fracture of interfaces, damage detection, and residual life assessment of aged concrete structures and structural rehabilitation.

ACI member **Victor E. Saouma** is a professor in the Department of Civil, Environmental, and Architectural Engineering at the University of Colorado at Boulder. He is a member of ACI Committee 446, Fracture Mechanics, and Joint ACI-ASCE Committee 447, Finite Element Analysis of Reinforced Concrete Structures. His research interests include experimental and numerical fracture mechanics, dam engineering, and fiber optics-based sensors.

several points in the softening portion of the curve to measure the compliance. The compliance measurements were taken only for the last six specimens.

### Evaluation of specific fracture energy

The specific fracture energy  $G_F$  was obtained from the area under the overall splitting force  $F_s$  versus the CMOD curve divided by the projected fracture area (ligament length times width). The influence of the self-weight on the fracture energy is negligible, which is an important advantage compared with the three-point bending test where the fracture energy part due to the self-weight of the beam, in the case of concrete, can amount to 40 to 60% of the total fracture energy. Table 1

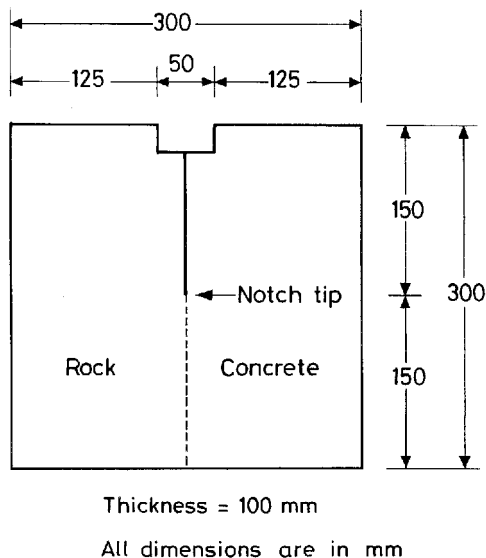


Fig. 1—Geometry of limestone-concrete wedge splitting specimen.

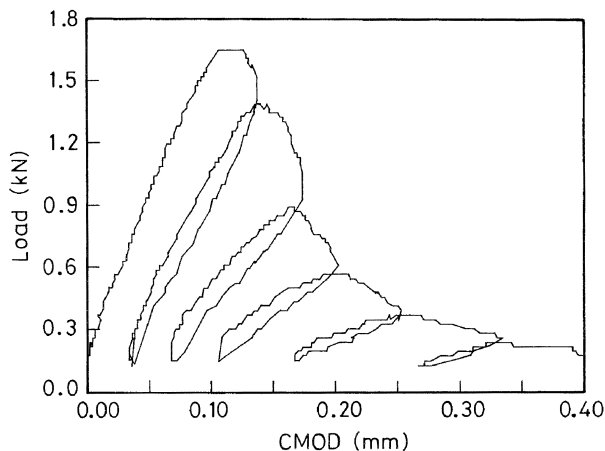


Fig. 2—Vertical load versus CMOD curve (Test 7).

shows the mean value of fracture energy obtained from different specimens. Figure 3 shows the vertical load plotted against the CMODs for different material contacts. The maximum splitting load and fracture energy for solid concrete, solid limestone,<sup>5</sup> and limestone-concrete contacts are shown in Table 2. It should be mentioned that the crack started at the notch and propagated all along the interface and, hence, the fracture energy measured is that of the interface.

### NUMERICAL ANALYSIS OF LIMESTONE-CONCRETE WEDGE-SPLITTING SPECIMEN

The wedge-splitting specimens were analyzed numerically using the finite element code MERLIN.<sup>6</sup> Both linear and non-linear-based fracture mechanics analyses were performed.

### Linear elastic fracture mechanics analysis

The fracture at a bimaterial interface is in mixed mode even when the loading is pure Mode I and the geometry of the specimen symmetric with respect to an existing crack. Hence, the main objective of doing the linear elastic fracture mechanics (LEFM) numerical simulations was to determine the fracture toughness in Modes I and II, respectively, when subjected to Mode I type loading, for the limestone-concrete interface.

The compliance method<sup>7</sup> is used in the analysis of the wedge-splitting specimens, wherein an effective crack length  $a_{eff}$ , which is longer than the true crack but shorter than the true crack, plus the fracture process zone (Fig. 4), is determined by finite element calibration. A series of analyses

Table 1—Mode I fracture energy for limestone-concrete specimen

	$F_{v,max}$ , kN	$G_F$ , N/m
Mean value	1.52	38.33
Standard deviation	0.20	6.66

Table 2—Fracture energy for different material contacts

	$F_{s,max}$ , kN (kips)	$G_F$ , N/m (lb/in.)
Solid concrete	4.59 (1.03)	181.6 (1.037)
Solid limestone	3.75 (0.84)	37.4 (0.214)
Limestone-concrete	2.84 (0.64)	38.3 (0.219)

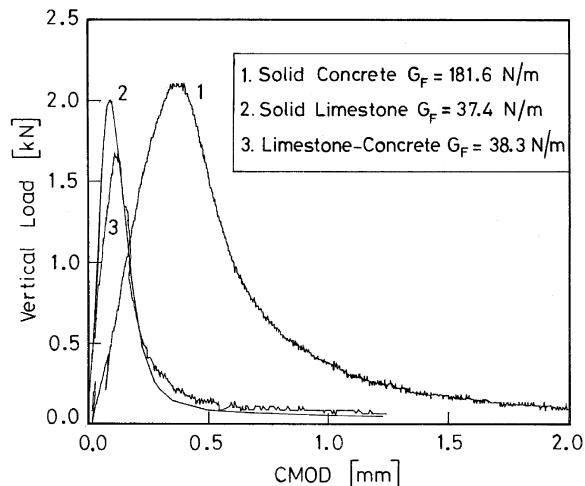


Fig. 3—Vertical load versus CMOD curves for different material contacts.

with different crack lengths, starting with the initial notch, were performed. In these analyses, the ratio of elastic modulus of concrete to limestone was taken to be 0.80, which is determined experimentally. From each analysis, the compliance and the stress intensity factors were determined in terms of the crack length. The stress intensity factors were determined using the Stern contour integral,<sup>8</sup> which accounts for the presence of oscillatory singularity and implemented in MERLIN for bimaterial bodies. The numerical compliance curve that was obtained is shown in Fig. 5. For each test, the effective modulus of elasticity is determined using the relation<sup>7</sup>

$$E_{eff} = \frac{C_n^o}{C_{exp}^o} \quad (1)$$

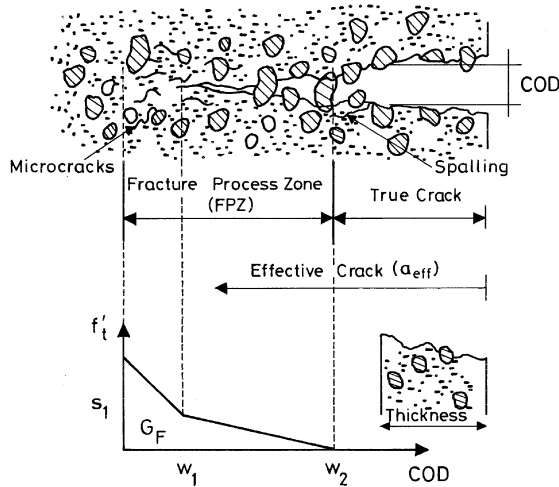


Fig. 4—Effective crack length.

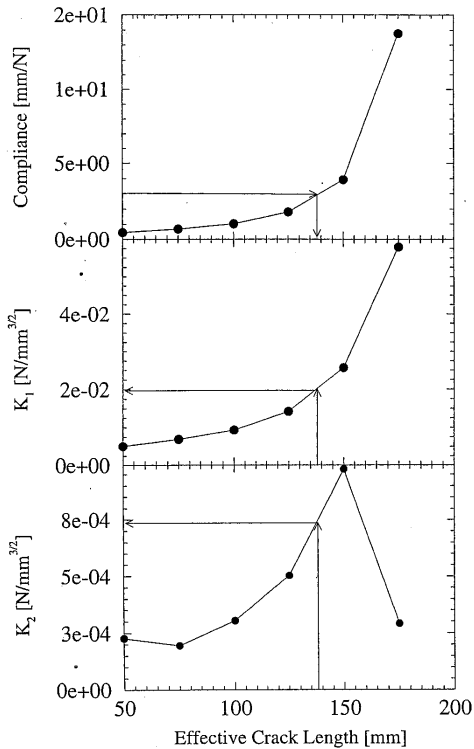


Fig. 5—Numerical compliance curve and unit load stress intensity factors for concrete-limestone specimen.

where  $C_n^o$  is the initial numerical compliance of the notched specimen without crack, and  $C_{exp}^o$  is the initial compliance of the experimental splitting load versus CMOD curve. In doing so, the finite element calibration resulted in a normalized compliance  $C_n$  equal to

$$C_n = E_{eff} C_{exp} \quad (2)$$

In the experiments, a series of unload/reload versus CMOD readings were recorded as shown in Fig. 2. From these unload/reload cycles, the experimental compliance was measured and the numerical compliance computed using Eq. (2). Using the compliance curve shown in Fig. 5, the effective crack length was extracted. The positions of the crack tip in the specimen at the locations of compliance measurements are shown in Fig. 6. Using the value of effective crack length, the stress intensity factors  $K_1$  and  $K_2$  were obtained from SIF curves shown in Fig. 5. These SIF curves were obtained for unit load and different notch lengths. In this procedure, through a linear regression, the following relations are numerically approximated

$$a_{eff} \approx a_{eff}(C_n) \quad (3)$$

$$K_1 \approx K_1(a_{eff}) \quad (4)$$

$$K_2 \approx K_2(a_{eff}) \quad (5)$$

where  $a_{eff}$  is the crack length. The stress intensity factors  $K_{1c}$  and  $K_{2c}$ , obtained as functions of the effective crack length, are shown in Fig. 7. The  $K_{1c}$  and  $K_{2c}$  values obtained for each unload/reload cycle were considered and averaged to obtain  $K_{1c}$  and  $K_{2c}$  for the specimen, which are summarized in Table 3. In this table, the fracture toughness values for the first six tests are not shown because the compliance measurements (unload/reload) were not taken. The  $G_F$  values shown in this table were determined from the experimental load-CMOD response curves.

### Nonlinear fracture mechanics analysis

Nonlinear analysis was performed using the Interface Crack Model.<sup>9</sup> This is a discrete crack model, which was developed to simulate cracking in solid concrete and along rock-concrete interface, subjected to mixed mode load conditions. In

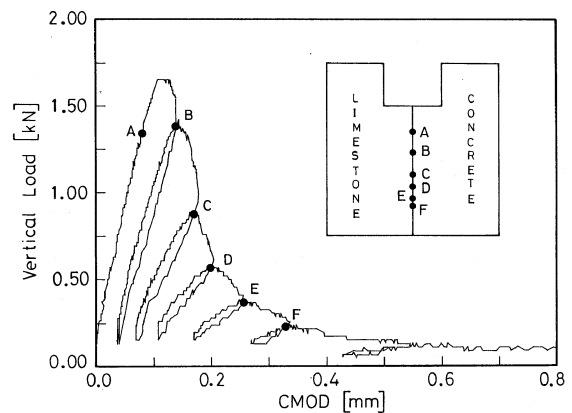


Fig. 6—Vertical load versus CMOD curve (experimental along with crack position obtained from LEM analysis (Test 7)).

this analysis, three-noded triangular elements were used for concrete and limestone. Interface elements were provided along the junction of concrete and rock. The analysis was carried out incrementally using displacement control, with displacements prescribed on either side of the notch. A hinged boundary condition was provided at the bottom of the interface. The analysis was carried out until failure, which occurred by the crack traveling all the way along the interface. Figure 8 shows the vertical load versus CMOD response curve obtained from this analysis.

**Table 3—Fracture energy (experimental) and stress intensity factors (analyses) for limestone-concrete wedge splitting specimens**

	Experimental		Numerical		
	$F_{v,max}$ , kN	$G_F$ , N/m	$K_{1c}$ , MPa/m	$K_{2c}$ , MPa/m	$G_c$ , N/m
Test 1	1.65	39.70	—	—	—
Test 2	1.47	30.36	—	—	—
Test 3	1.38	35.00	—	—	—
Test 4	1.32	36.78	—	—	—
Test 5	1.20	43.60	—	—	—
Test 6	1.32	30.18	—	—	—
Test 7	1.63	49.76	0.291	0.0102	3.30
Test 8	1.95	40.98	0.305	0.0106	3.33
Test 9	1.50	30.62	0.248	0.0085	2.20
Test 10	1.53	42.65	0.279	0.0100	2.78
Test 11	1.53	32.14	0.277	0.0097	2.75
Test 12	1.75	48.16	0.281	0.0100	2.83
Mean value	1.52	38.33	0.280	0.0100	2.87
Standard deviation	0.20	6.66	0.017	0.0007	0.38

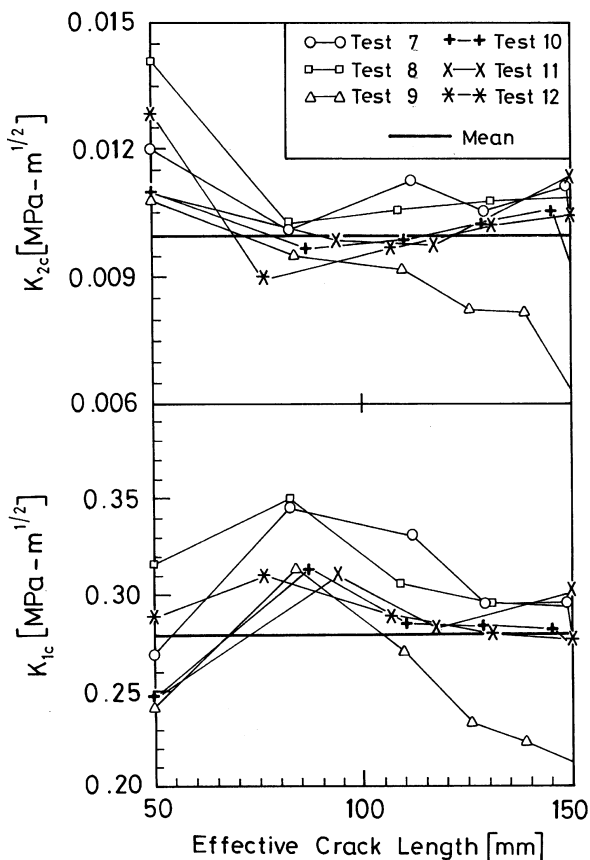


Fig. 7— $K_{1c}$  and  $K_{2c}$  as function of effective crack length.

## APPLICATION TO GRAVITY DAMS

All concrete dams suffer from cracking, which is caused by various factors such as construction, curing, alkali-aggregate reaction, and load application. Of greater concern are those cracks that develop as a result of hydrostatic load application, leading to significant change in the failure resistance of the structure. Due to this growing concern, concrete dams are increasingly becoming scrutinized by regulatory agencies that are responsible for dam safety.<sup>10</sup>

Despite the tremendous progress made to conduct sophisticated finite element analysis, the design and rehabilitation of dams are frequently based on the simple Bernoulli's equation ( $P/A + Mc/I = 0$ ). Such an equation, valid only for shallow beams, cannot be uncritically applied to a dam without certain shear corrections; furthermore, it fails to recognize the singular nature of the stress at the tip of a crack. Hence, it is necessary to move away from the simple analytical approaches that evolved during the heyday of dam construction and apply the recent and rational developments of fracture mechanics and finite element formulations.

It is well recognized that the primary mode of failure in a gravity dam is sliding (rather than overturning) along the uncracked ligament. Hence, most agencies require evaluation of the shear friction factor (SFF) defined by

$$SFF = \frac{cL + \Sigma V \tan \phi}{\Sigma H} \quad (6)$$

where  $c$  is the cohesive strength;  $L$  is the uncracked ligament length;  $\Sigma V$  is the resultant vertical force;  $\phi$  is the angle of internal friction; and  $\Sigma H$  is the resultant horizontal force. It is noted that cohesion is allowed for the shear strength but no tensile stresses are permitted. Hence, there is a significant inconsistency between the assumptions made for the crack length determination and sliding safety factor calculations. The fracture properties extracted previously were used in the analysis of the Greyrock gravity dam that has been targeted for major rehabilitation for the determination of the crack length. It is assumed that the fracture properties obtained from small specimens are applicable to large structures and size effect is not considered in this work.

### Description of Greyrock Dam

The Greyrock Dam is a gravity-type dam built across the Kanawha River basin in West Virginia during the 1930s. It is

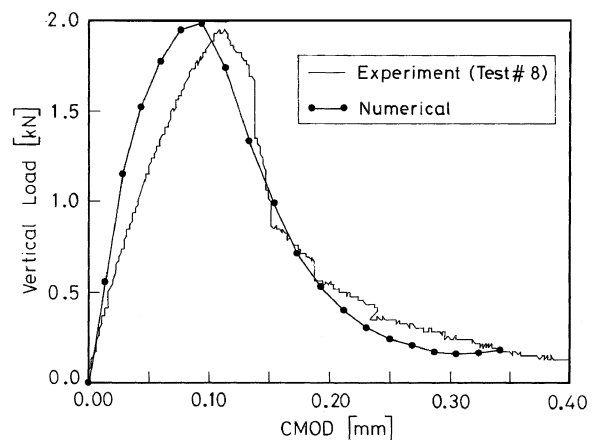


Fig. 8—Comparison of experimental and numerical vertical load versus CMOD curve.

176 ft (53.7 m) high and has 53 monoliths, with a crest elevation of 1525 ft (464.8 m). Based on hydrological studies by the U.S. Army Corps of Engineers, using classical equilibrium analysis, it was determined that the probable maximum flood (PMF) elevation is at 1555.8 ft (474.2 m) and the imminent failure flood (IFF), which is the pool elevation that would trigger failure, is at 1533 or 22 ft (467.3 or 6.71 m) below the PMF. Hence, this dam has been targeted for major rehabilitation.<sup>11</sup> The cross section of the dam along with the dimensions is shown in Fig. 9. Table 4 gives the material properties of the concrete dam, rock foundation, and the interface.

### LEFM analysis of Greyrock Dam

In LEFM analysis, the crack length along the interface between the concrete dam and rock foundation was determined by using the concepts of bimaterial fracture mechanics, which considers the oscillatory nature of the stress singularity at the crack tip.

A series of LEFM analyses were performed with different crack lengths. In all of the analyses, the U.S. Army Corps of Engineers determined IFF elevation of 1533 ft (467.3 m) was used because the classical analysis<sup>11</sup> had yielded this water elevation to trigger failure. The stress intensity factors  $K_1$  and  $K_2$  in Mode I and Mode II, respectively, were computed using the Stern contour integral for bimaterial interfaces in MERLIN. The following loads were used in the analysis:

1. Hydrostatic load with water elevation at 1533 ft (467.3 m);
2. Body forces due to the self-weight of the dam; and
3. Full uplift pressure inside the crack.

### Results of LEFM analysis

Figure 10 illustrates the variation of the Mode I stress intensity factor, Mode II stress intensity factor, and the energy release rate with crack length. In this figure, it is seen that the energy release rate is constant until a crack length of 33 ft (10 m) after which it starts to increase. This implies that the crack remains within the interface up to a length of 33 ft (10 m) and departs away from it thereafter. Using the traditional criteria of  $K_{Ic} = 0$ , the crack length obtained is 65 ft (19.8 m). From Table 3, the critical fracture toughness for the limestone-concrete interface was obtained as 248 psi/in. (0.28 MPa/m). With this value, a crack length of 56 ft (17 m) was obtained. This indicates that predicting a crack length based on zero fracture toughness is very conservative.

### Nonlinear fracture mechanics analysis (NLFM) of Greyrock Dam

Contrary to the LEFM analysis wherein all the energy is transferred at the crack tip, in a nonlinear fracture mechanics

**Table 4—Material properties of Greyrock Dam**

Concrete	
Weight density	150 lb/ft <sup>3</sup> (23.6 kN/m <sup>3</sup> )
Elastic modulus	4.867 E06 psi (33.54 GPa)
Poisson's ratio	0.255
Rock	
Weight density	0
Elastic modulus	3.952 E06 psi (27.23 GPa)
Poisson's ratio	0.165
Interface	
Cohesion	42 psi (0.289 MPa)
Angle of friction	51 degrees

(NLFM) analysis, energy is also transferred along the crack. The Interface Crack Model<sup>9</sup> is used in the NLFM analysis. The criterion for crack propagation was strength-based, in which the major principal stress cannot exceed the tensile strength. Interface elements are provided along the rock-concrete joint. These elements are capable of modeling the shear failure along the interface and may fail either due to crack opening or excessive shear stresses. The analysis was carried out by incrementally increasing the water elevations, with the first increment being the gravity dead load. Other load increments were water elevations starting from a low value of 50 ft (15.3 m) and increasing in increments of 50 ft (15.3 m) until the imminent failure flood level, as determined from classical equilibrium analysis, was obtained. Thereafter, each increment was increased by 1 ft (0.31 m) until the probable maximum flood level was reached. The incremental load size was reduced for the accuracy in predicting the crack profile and to achieve faster convergence of the nonlinear solution. Crack kinking was considered in the direction perpendicular to the direction of maximum principal stress. The fracture energy in Mode I for the interface and the kinked crack was considered to be the same because the crack kinks into the rock and the Mode I fracture energy obtained experimentally for rock and the interface were almost the same, as illustrated in Fig. 3.

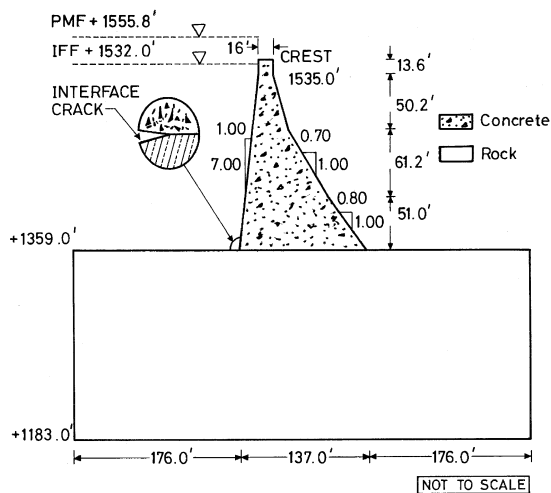


Fig. 9—Simplified geometry of Greyrock Dam.

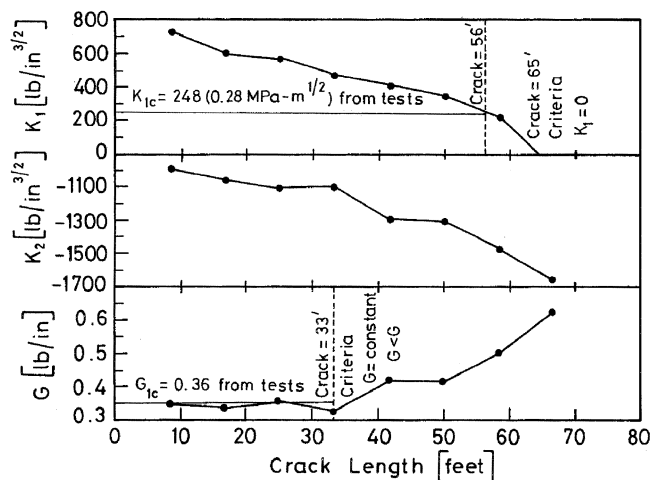


Fig. 10—Stress intensity factors and fracture energy versus crack length.

## Results of the NLFM analysis

Figure 11 shows the final crack profile with respect to changing water elevations. It is seen that the crack, which remains within the interface for 8.3 ft (2.5 m) (Point A), started to kink into the adjoining rock when the water elevation was at 175 ft (53.4 m). This elevation was 1 ft (0.31 m) above the IFF level determined from the classical equilibrium method. The kinked crack propagated alone until the water elevation reached 184 ft (56.1 m). At this point, the crack branched out, that is, the interface crack started to propagate again. When the water reached 190.8 ft (58.2 m) (which is 8 ft [2.4 m] below the PMF), the nonlinear solution failed to converge due to the presence of high shear stresses. This indicated final failure due to sliding.

## CONCLUSIONS

### Wedge splitting bimaterial tests

The following qualitative conclusions are made from the wedge splitting tests performed on limestone-concrete interface specimens:

1. As seen from Table 2, it is remarkable that the maximum splitting load for the bi-material specimens reached nearly 61% of the solid concrete specimen, whereas the fracture energy amounted to only 21% of the value obtained for concrete. This shows that the difference in the behavior of the interface as compared with the intact material lies basically in the postpeak response, as seen in Fig. 3. This implies that the consideration of the strength parameter alone is not adequate in the safety assessment of massive concrete structures. In addition to strength, the fracture energy has to be taken into account;

2. The interface demonstrated significant prepeak non-linearity because of prepeak cracking and damage. The specimens failed along the interface through its center. The loading-unloading curves in Fig. 2 showed large-scale degradation of the unloading modulus; and

3. Table 5 shows a comparison of the fracture energy obtained in the limestone/concrete specimen with those of other interfaces determined by other investigators. It can be concluded from this table that the fracture energy in Mode I for interfaces fall within a respectful range.

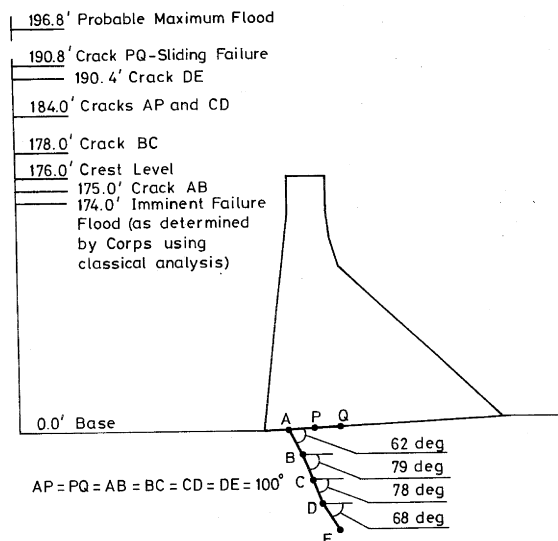


Fig. 11—Final crack profile with respect to changing water elevations.

## Numerical analysis

The following conclusions are made from the results of the numerical analyses on wedge splitting specimens:

1. The curves of  $K_1$  and  $K_2$  versus the effective crack length showed a plateau, which was also observed in solid limestone specimens.<sup>7</sup> This is synonymous with steady crack propagation that indicates that objective  $K_1$  and  $K_2$  values were obtained;

2. As tabulated in Table 6, the Mode I fracture toughness of the limestone-concrete interface was found to be 0.28 MPa/m as compared with 0.80 MPa/m for solid limestone and 1.04 MPa/m for solid concrete.<sup>7</sup> This implies that the resistance offered by a limestone-concrete interface to crack propagation is only 27% of that offered by intact concrete and 35% of intact limestone;

3. The Mode II fracture toughness under pure Mode I load conditions for the limestone-concrete interface was obtained as 0.01 MPa/m. This value is relatively low because of the absence of any shear because the specimen was subjected to pure Mode I loading;

4. As seen from Fig. 6, the crack was initiated at the notch tip because of stress concentration, and this cracking was responsible for the nonlinear behavior of the ascending part of the load-CMOD curve. Steady crack propagation and, hence, the formation of a small process zone in front of the crack tip as it propagates along the interface, leads to the softening behavior in the postpeak response;

5. The resistance offered by limestone-concrete interface to crack propagation in Mode I was only 27% of concrete and 35% of solid limestone. This may be due to the absence of interlock mechanism as found in concrete leading to the formation of smaller process zone in front of the true crack. This may also be the reason for the steep postpeak behavior of limestone-concrete interface as compared with solid concrete interface; and

6. From Fig. 8, it is seen that the interface crack model adequately captures the maximum load and the postpeak behavior, but the initial stiffness is overestimated.

### Analysis of Greyrock Dam

The following conclusions are made from the analysis of Greyrock Dam:

Table 5—Comparison of fracture energy for different interfaces

Source	$G_F$ , N/m
<i>Present work</i> Limestone-concrete	38.3
<i>Lee, Buyukozturk, and Kitsutaka</i> <sup>12</sup> Low-strength mortar-granite High-strength mortar-granite	25 to 56 62 to 97
<i>Yan and Mindess</i> <sup>13</sup> 0.5% steel fiber-concrete 1.0% steel fiber-concrete 0.5% polypropylene-concrete 1.0% polypropylene-concrete	54 to 65 71 to 86 40 to 45 40 to 45

Table 6—Fracture toughness for different material contacts

	$K_{1c}$ , MPa/m (ksi/in.)	$K_{2c}$ , MPa/m (ksi/in.)
Solid concrete	1.04 (0.95)	—
Solid limestone	0.80 (0.73)	—
Limestone-concrete	0.28 (0.26)	0.01 (0.009)

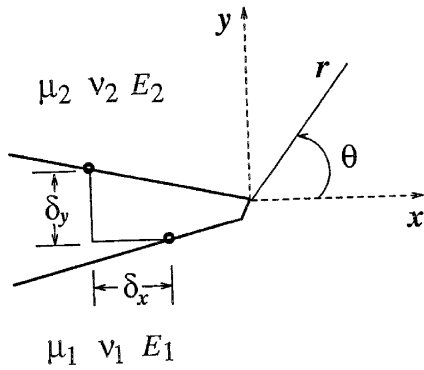


Fig. 12—Geometry and conventions of interface crack.

1. The LEFM analysis, considering the bimaterial nature of the interface, yielded a crack length of 35 ft (10.7 m). The classical equilibrium analysis estimated the crack length to 65 ft (19.8 m). The NLFM analysis yielded a total crack length of 25 ft (7.6 m) in the interface and 33 ft (10 m) into the rock. These indicate that the classical equilibrium analysis highly overestimates the crack length, thus making the rehabilitation scheme (if needed) an un-economical process; and

2. The NLFM analysis indicates a shorter crack length within the interface. This is due to the closure of interface crack due to full uplift pressure in the kinked crack.

### ACKNOWLEDGMENTS

The authors would like to thank V. Slowik, Professor at the Hochschule für Technik, Wirtschaft, und Kultur Leipzig (FH), Germany, for the assistance rendered in the experimental program of this work.

### NOTATION

$a_{eff}$	=	effective crack length
CMOD	=	crack mouth opening displacement
$C_n$	=	normalized compliance
$C_n^{exp}$	=	initial compliance of experimental load-CMOD curve
$C_n^o$	=	initial numerical compliance of notched specimen
FPZ	=	fracture process zone
$F_s$	=	splitting force
$F_{s,max}$	=	maximum splitting force
$G_F$	=	specific fracture energy
$G_F^I$	=	fracture energy in Mode I
$G_{Ic}$	=	Mode I fracture toughness of interface material
$K_1$	=	Mode I stress intensity factor of interfacial crack
$K_2$	=	Mode II stress intensity factor of interfacial crack
$K_{1c}$	=	Mode I fracture toughness of interface material
$K_{2c}$	=	Mode II fracture toughness of interface material when subjected to Mode I loading

### REFERENCES

1. Saouma, V. E.; Boggs, H.; and Morris, D., "Safety Assessment of Concrete Dams Using Fracture Mechanics," *Proceedings of the 18th ICOLD (International Commission on Large Dams) Conference*, Durban, South Africa, 1994, pp. 1415-1435.
2. Federal Energy Regulatory Commission, "Engineering Guidelines for the Evaluation of Hydropower Projects," Office of Hydropower Licensing, 1991.
3. Bruhwiler, E., and Wittmann, F., "The Wedge Splitting Test, A Method of Performing Stable Fracture Mechanics Tests," *Engineering Fracture Mechanics*, V. 35, 1990, pp. 117-126.
4. Chandra Kishen, J. M., "Interface Cracks: Fracture Mechanics Studies Leading Towards Safety Assessment of Dams," PhD thesis, Department of Civil, Environmental, and Architectural Engineering, University of Colorado, Boulder, Colo., June 1996.

5. Bruhwiler, E.; Broz, J.; and Saouma, V. E., "Fracture Model Evaluation of Dam Concrete," *Journal of Civil Engineering Materials*, ASCE, V. 3, No. 4, Nov., 1991, pp. 235-251.
6. Reich, R.; Cervenka, J.; and Saouma, V. E., "MERLIN, A Three-Dimensional Finite Element Program Based on a Mixed-Iterative Solution Strategy for Problems in Elasticity, Plasticity, and Linear and Nonlinear Fracture Mechanics," EPRI, Palo Alto, Calif., 1997, <http://civil.colorado.edu/~saouma/merlin>.
7. Bruhwiler, E., and Saouma, V. E., "Fracture Testing of Rock by the Wedge Splitting Test," *Proceedings of the 31st U.S. Symposium on Rock Mechanics*, Golden, Colo., 1990, pp. 287-294.
8. Hong, C. C., and Stern, M., "The Computation of Stress Intensity Factors in Dissimilar Materials," *Journal of Elasticity*, V. 8, No. 1, 1978, pp. 21-34.
9. Cervenka, J.; Chandra Kishen, J. M.; and Saouma, V. E., "Mixed Mode Fracture of Cementitious Bimaterial Interfaces—Part II: Numerical Simulation," *Engineering Fracture Mechanics*, V. 60, No. 1, 1998, pp. 95-107.
10. Saouma, V. E.; Dugar, R.; and Morris, D., "Proceedings Dam Fracture," Electric Power Research Institute, Palo Alto, Calif., Sept. 1991.
11. U.S. Army Corps of Engineers, "Dam Safety Assurance Program Evaluation Report," Three Volumes, 1994.
12. Lee, K. M.; Buyukozturk, O.; and Kitsutaka, Y., "The Role of Interfacial Fracture Toughness in Cracking Behavior of High-Strength Concrete," *Interface Fracture and Bond*, SP-156, O. Buyukozturk and M. Wecharatana, eds., American Concrete Institute, Farmington Hills, Mich., 1995, pp. 69-84.
13. Yan, C., and Mindess, S., "Fracture Mechanics Analysis of Bond Behaviour Under Dynamic Loading," *Interface Fracture and Bond*, SP-156, O. Buyukozturk and M. Wecharatana, eds., American Concrete Institute, Farmington Hills, Mich., 1995, pp. 107-123.
14. Hutchinson, J. W., and Suo, Z., "Mixed Mode Cracking in Layered Materials," *Advances in Applied Mechanics*, V. 29, 1992, pp. 63-191.
15. Carlsson, L. A., and Prasad, S., "Interfacial Fracture of Sandwich Beams," *Engineering Fracture Mechanics*, V. 44, 1993, pp. 581-590.
16. Dundurs, J., "Edge-Bonded Dissimilar Orthogonal Elastic Wedges Under Normal and Shear Loading," *Journal of Applied Mechanics*, V. 36, 1969, pp. 650-652.

### APPENDIX

#### Stress and displacement fields for cracks between dissimilar materials

Considering the bimaterial interface crack in Fig. 12 for traction-free plane problems, the near-tip normal and shear stresses  $\sigma_{yy}$  and  $\tau_{xy}$  may conveniently be expressed in complex stress intensity factors<sup>14,15</sup>

$$\sigma_{yy} + i\tau_{xy} = \frac{(K_1 + iK_2)r^{\varepsilon}}{\sqrt{(2\pi r)}} \quad (7)$$

where  $i = \sqrt{-1}$ ,  $K_1$  and  $K_2$  are components of complex stress intensity factor  $K = K_1 + iK_2$ .

In the previous equations,  $\varepsilon$  is the oscillation index given by

$$\varepsilon = \frac{1}{2\pi} \ln \left( \frac{1-\beta}{1+\beta} \right) \quad (8)$$

where  $\beta$  is one of Dundur's elastic mismatch parameters,<sup>16</sup> which for plane strain is given by

$$\beta = \frac{\mu_1(1-2\nu_2) - \mu_2(1-2\nu_1)}{2[\mu_1(1-\nu_2) + \mu_2(1-\nu_1)]} \quad (9)$$

in which  $\mu$ ,  $\nu$ , and  $a$  are the shear modulus, Poisson's ratio, and crack length, respectively, and subscripts 1 and 2 refer to the materials above and below the interface, respectively.